AD-A194 418 EXPERIMENTAL ASPECTS OF USING TIME-AVERAGED HOLOGRAPHIC 1/1
INTERFEROMETRY IO. (U) AERONAUTICAL RESEARCH LABS
MELBOURNE (AUSTRALIA) S J RUMBLE 25 AUG 87
UNCLASSIFIED ARL-STRUC-IM-467 DODA-AR-004-549 F/G 11/4 NL

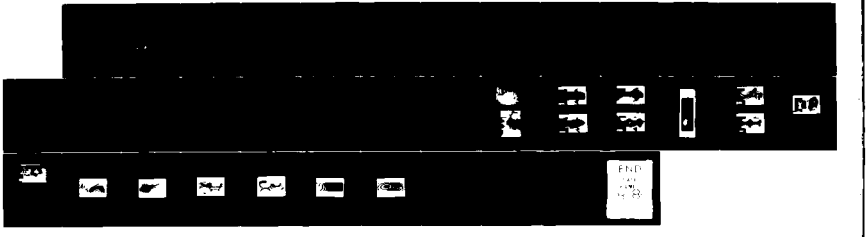

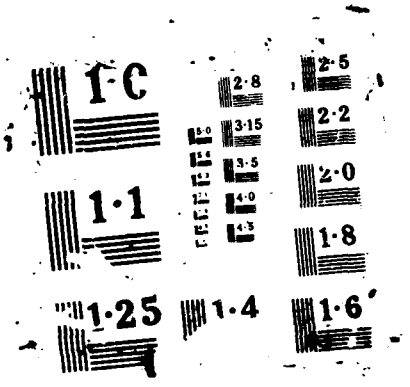
1·C
1·1
1·25
2·8
3·15
3·5
4·0
1·4
2·5
2·2
2·0
1·8
1·6

ARL-STRUC-TM-467

AR-004-549

DEPARTMENT OF DEFENCE

DEFENCE SCIENCE AND TECHNOLOGY ORGANISATION

AERONAUTICAL RESEARCH LABORATORIES

MELBOURNE, VICTORIA

Structures Technical Memorandum 467

EXPERIMENTAL ASPECTS OF USING TIME-AVERAGED HOLOGRAPHIC INTERFEROMETRY TO DETECT BARELY VISIBLE IMPACT DAMAGE IN A GRAPHITE/EPOXY COMPOSITE PLATE (U)

by

S.J. RUMBLE

Approved for public release.

AR-004-549

DEPARTMENT OF DEFENCE
DEFENCE SCIENCE AND TECHNOLOGY ORGANISATION
AERONAUTICAL RESEARCH LABORATORIES

Structures Technical Memorandum 467

EXPERIMENTAL ASPECTS OF USING TIME-AVERAGED HOLOGRAPHIC INTERFEROMETRY TO DETECT BARELY VISIBLE IMPACT DAMAGE IN A GRAPHITE/EPOXY COMPOSITE PLATE (U)

by

S.J. Rumble

SUMMARY

Time-averaged holographic interferometry has been used to detect barely visible impact damage in a graphite/epoxy plate. Details are given of both the experimental and theoretical aspects of time-averaged holographic interferometry, including temporal modulation of the laser light. Double exposure holographic interferometry has also been used to detect barely visible impact damage.

POSTAL ADDRESS: Director, Aeronautical Research Laboratories,
P.O. Box 4331, Melbourne, Victoria, 3001, Australia

CONTENTS

1. INTRODUCTION

Graphite/epoxy composite materials are increasingly being used to improve aircraft structural design. However, the material can suffer a form of damage termed 'barely visible impact damage' (BVID), which can degrade the properties of the material. In this type of damage, there can be significant delaminations, even though externally only a very small indentation is visible. In a recent paper, Heller and Rumble (1) investigated the potential for characterising the dynamic response of a graphite/epoxy plate to indicate the presence and possibly the location of BVID. The work included measurements of the natural frequencies and modal dampings using accelerometer response, and determination of mode shapes using time-averaged holographic interferometry. This paper provides more detail of the experimental and theoretical aspects of the time-averaged holographic interferometry referred to above. It also includes an extension of the holographic interferometry (HI) work to temporal modulation of the laser light used in recording holograms, and double exposure holographic interferometry using thermal stress to induce deformations.

2. HOLOGRAPHIC INTERFEROMETRY

Holographic interferometry (HI) utilizes the ability of holography to store and recreate the optical fields of an object. This enables the interferometric comparison of the optical fields of an object which occurred at different times and with the object in different states. A more detailed introduction to the general theory of holography and HI has been given by Rumble (2) and has also been presented in numerous texts (3-5).

The fundamental result of HI theory, for the case where two object fields are stored (double exposure HI), is that the phase difference $\delta\phi$ between the optical fields from the same point Q on the object, is related to the displacement $\underline{d}$ of the point as follows:

$$\delta\phi = \underline{K} \cdot \underline{d} \qquad (1)$$

where $\underline{K}$ is a vector defined by the optical arrangement used to illuminate and view the object as shown in Figure 1. If the object was illuminated from a direction

$\underset{\sim}{k}_1$, and is later viewed through the hologram from a direction $\underset{\sim}{k}_2$ then the vector $\underset{\sim}{K} = \underset{\sim}{k}_2 - \underset{\sim}{k}_1$ and is termed the sensitivity vector. The vectors $\underset{\sim}{k}_1$ and $\underset{\sim}{k}_2$ are the propagation vectors of the incident and scattered light and both have magnitudes of $2\pi/\lambda$, where λ is the wavelength of the laser light used. The actual intensity at the point Q in the reconstructed image will depend on the relative intensities of the two optical fields at Q and the phase difference $\delta\phi$.

3. TIME-AVERAGED HOLOGRAPHIC INTERFEROMETRY

The fundamental result given above can be extended to include the case of a vibrating object where the displacement $\underset{\sim}{d}(l,m)$ of a general point Q(l,m) on the object's surface is varying as a sinusoidal function of time as follows

$$\underset{\sim}{d}(l,m,t) = \underset{\sim}{d}_o(l,m)\sin(\omega t + \phi_o), \tag{2}$$

where $\underset{\sim}{d}_o$ is the amplitude of a vibrational mode with angular frequency ω.

In this case, as shown in Appendix I, the intensity I(l,m) in the reconstructed image can be written as follows:

$$I(l,m) = I_o(l,m)J_o^2[\underset{\sim}{K} \cdot \underset{\sim}{d}_o(l,m)], \tag{3}$$

where I_o is the intensity of the stationary object and J_o is the zero-order Bessel function of the first kind.

The J_o^2 term leads to the formation of fringes over the object's surface. The fringes form contours of equal levels of the peak to peak displacement of the object's surface during vibration in a given mode. The maximum of J_o^2 at $\underset{\sim}{K} \cdot \underset{\sim}{d}_o(l,m) = 0$ corresponds in general to the zero displacement or nodal points, and hence nodes can easily be identified as the brightest fringes.

The contoured images created in this form of time-averaged HI do not give information about the phase relationships between points in the vibrating object. However, this information can be obtained if the optical phase of the reference beam is sinusoidally modulated at the same frequency as the vibrating object. It is shown in Appendix I that in this case the intensity I(l,m) in the reconstructed image has the form

$$I(l,m) = I_o(l,m)J_o^2[((\underset{\sim}{K} \cdot \underset{\sim}{d}_o(l,m))^2 + \phi_{ro}^2 - 2\underset{\sim}{K} \cdot d_o(l,m)\phi_{ro}\cos\Phi_o(l,m))^{1/2}], \tag{4}$$

where ϕ_{ro} is the amplitude of the optical phase modulation, and $\Phi_o(l,m)$ is the phase difference between the reference beam optical phase modulation and the vibrational phase at the point Q(l,m).

If the vibrating object has only two phases (Φ_o = 0° and 180°) then the argument of the Bessel function reduces to $\underset{\sim}{K} . \underset{\sim}{d}_o(l,m) - \phi_{ro}$ for 0° and $\underset{\sim}{K} . \underset{\sim}{d}_o(l,m) + \phi_{ro}$ for 180°. The brightest fringe on the image will now occur where $\underset{\sim}{K} . \underset{\sim}{d}_o(l,m) \pm \phi_{ro} = 0$. Hence the bright fringes that were located at vibrational nodes on an image recorded without phase modulation, will have moved towards some anti-nodes and away from the others in an image recorded with optical phase modulation. Further discussion of the use of temporal modulation techniques in HI to determine the phase of vibration objects can be found in references 3,6-8.

4. SPECIMEN

In this work, time-averaged HI was performed on a graphite/epoxy composite plate, vibrating in a cantilever arrangement. The specimen had a material designation of XASfibre/914 resin. The layup of the plate was $(\pm 45/0_2)_{3s}$ and its in plane dimensions were 73mm x 225mm with a thickness of approximately 2.9mm. The specimen was inspected using an ultrasonic C-scan before testing to confirm that it was undamaged.

5. HOLOGRAPHIC PROCEDURE

The optical arrangement used to record the time-averaged holograms is shown in Fig. 2. The limited optical bench space available, and the size of the specimen necessitated the use of two plane mirrors to gain maximum expansion and hence uniformity of the specimen and reference illumination beams. The holograms were recorded on Agfa 8E56 holographic plates using the 514.5nm green line from an argon laser. A one to one ratio between the reference and specimen intensities at the plate was used. The 8E56 plates were exposed for three seconds, which would have corresponded to ND2 to ND2.5 after fixing. However, in this work, phase holograms were created using a reversal bleach technique. The holograms were photographed using Ilford FP4 film. The film was processed in Ilford PQ universal developer to give maximum contrast.

6. EXCITATION PROCEDURE

The specimen was firmly clamped at one end as shown in Figs 3 and 4, and a sinusoidally varying excitation force was applied laterally at the free end. The dynamic response of the specimen was determined using a small accelerometer (PCB309-A) attached near the free end. The excitation force was supplied by a Ling 409 electro-magnetic shaker which was initially driven by an ARL high output impedance amplifier connected to the 0 degree output of a Muirhead D-88-A two phase oscillator. In later tests, problems with the amplifier necessitated the removal of the ARL amplifier and use of the oscillator to directly drive the shaker thus resulting in lower available excitation levels.

The 90 degree output from the oscillator and the accelerometer response were displayed in X-Y mode on an oscilliscope. Observation of the accelerometer response on this display, as the frequency was varied, enabled the determination of the modal frequencies. The voltage levels were used to calculate the peak to peak displacements of the specimen at the accelerometer using the relationship $x = a/\omega^2$, where x is the displacement, a the acceleration and ω the angular frequency of the vibration.

During the tests the excitation force was coupled to the specimen in a variety of ways. Initially a pushrod with an approximately 1cm diameter ball at its end was glued to the specimen with Araldite. Results obtained with this arrangement are shown in Figs. 5-8.

7. EXPERIMENTAL DIFFICULTIES

To investigate the sensitivity of the experimental arrangement to the clamping and excitation conditions, the specimen was removed and replaced. During removal, it was noted that the Araldite bond had weakened considerably. After replacement of the specimen and using a firm Araldite bond further attempts to record time-averaged holograms were unsuccessful. At this stage a number of excitation coupling techniques were attempted, including the use of wax, and high viscosity ultrasonic shear wave coupling fluid as the bonding between the 1cm ball and the specimen. Also a direct coupling between the pushrod and the specimen was attempted (shown in Fig. 4). Again attempts to record time-averaged holograms were unsuccessful.

The problem was resolved when it was recognized that the amplifier output had a small 50Hz component and hence the specimen was being driven at 50Hz as well as the oscillator frequency. A 50Hz component had been observed in the frequency spectrum of the accelerometer signal. However this signal had been discounted as being due to direct 50Hz interference in the accelerometer leads and preamplifier. Removal of the amplifier, and the use of the oscillator to directly drive the shaker which was directly coupled via the pushrod to the specimen, enabled good quality time-average holograms to be recorded.

8. *DAMAGED SPECIMEN*

The tests proceeded to the next stage in which barely visible impact damage was produced in the specimen. The impact damage was imparted on the back face of the specimen using an ARL impact rig to drop a 9kg impactor from a height of 0.5m on to the specimen which was firmly clamped in a support structure. The amount of damage was determined using an ultrasonic C-scan. The result of this scan is shown in Fig. 9. This figure shows the damage in a plane at 0.9 of the thickness from the impacted face and this is the plane of maximum damage. The spanwise length of this damaged region was approximately 40mm, which constitutes a significant degree of damage. Time-averaged holograms of the damaged specimen were recorded for the vibrational modes with adequate response. These are shown in Figs. 10-12.

9. VIBRATIONAL PHASE DETERMINATION

The vibrational phase of the various regions in a number of modes were investigated using the technique of temporal modulation of the reference beam. The modulation was achieved by including in the optical path of the reference beam, a mirror mounted on a piezoelectric translator. The application of a voltage to the translator causes a movement of the mirror, and thus alters the reference beam path length and hence the relative optical phase of the reference beam at the holographic plate. The optical arrangement is shown in Figs. 13 and 14.

The electrical excitation system was arranged so that the electromagnetic shaker and translator could be driven at the same frequency but with a variable phase relationship. This was achieved by connecting the 0 degree phase output of a two phase Muirhead oscillator to a HP3314 function generator, which could be phase locked to the oscillator but with variable phase offset. The 90 degree output from

the oscillator drove the translator. The translator drive signal and the accelerometer response were monitored on a dual channel HP3582A Fourier analyser which enabled the phase difference between the two signals to be determined.

A number of holograms were recorded with different phase relationships between the exciting force and the temporal modulation of the reference beam, and also different amplitudes of movement of the translator. Examples of these holograms are shown in Figs. 15 to 18.

10. DOUBLE EXPOSURE HOLOGRAMS WITH THERMAL STRESSING

After the vibrational investigation of the damaged specimen, double exposure holograms were recorded on the front and back surface of the specimen. For these tests the specimen was heated to approximately 40°C and the first of the double exposure holograms was recorded. A second exposure was recorded on the same holographic plate, after a time lapse of approximately one minute. The results of these tests are shown in Figs. 19 and 20.

11. DISCUSSION

The photographs of the reconstructed images using time-averaged holography, shown in Figs. 5–8 and Figs. 10–12, clearly display fringes contouring the specimen. The relationship between the intensities of the bright fringes in these photographs are not representative of the actual intensities as the contrast has been improved in the photography stage.

For the illumination and viewing directions, and wavelength used in producing these images, the fringes contour points of equal displacement amplitude, with a contour interval of 0.3 micron. A quantitative examination of the modal shapes of the specimen was not performed.

The photographs of the time-averaged holograms for the damaged specimen, vibrating in modes with frequencies 1157 Hz, 2160 Hz, and 2340 Hz, are shown in Figs. 10–12. In Fig. 10, indication of the damaged region appears as a dark spot in an otherwise bright region. In Figs. 11 and 12, the indication of the damaged area appears as a perturbation of nearby fringes.

The effect of temporal phase modulation of the reference beam is shown in the comparison of Figs. 10,15 and 16. All these Figures show the specimen vibrating at 1157 Hz. Fig. 10 was recorded with no modulation. Both Figs. 15 and 16 were recorded with the same amplitude of optical phase modulation but with 180° phase difference between the optical phase modulation and the vibrational phase at the accelerometer. The region of the brightest fringe in Fig. 10 is occupied by a dark fringe in Figs. 15 and 16. In Fig. 15 the brightest fringes have moved to different regions when compared to Fig. 16. This indicates that these two regions were vibrating with a 180° phase difference. The contrast and appearance of the damaged region has also altered significantly in Figs. 15 and 16. Figs. 11,17 and 18 show similar behaviour to that discussed for Figs. 10,15 and 16 respectively. In this case the vibrational frequency was 2160 Hz.

In the double exposure holograms, shown in Figs. 19 and 20, the fringes contour points on the specimen which have the same projection of their displacements onto the sensitivity vector. The displacement of the points was caused by the thermal contraction of the specimen as it cooled from 40°C. In the vicinity of the damaged region the fringes are anomalous and clearly indicate the location of the damage.

At present the holographic techniques used in this work require extreme vibration isolation of the optical components and exposure in dark room conditions. This degree of vibration isolation is not required if a high power pulsed laser is used, and also exposures can be made in ordinary laboratory conditions. The development of a holographic system incorporating a pulsed laser is currently in progress. Further developments include the use of a photothermoplastic camera to perform real-time holography in which the fringes can be observed at the time of the experiment, and not after subsequent photographic processing and reconstruction of the holographic image. This enables the loading and excitation conditions to be varied so as to give the maximum amount of information. The capture of the fringe images using a diode array camera and subsequent computer processing can also result in the acquisition of more useful information. This can include the calculation of whole field strains over complex shapes.

12. CONCLUSIONS

The ability of holographic interferometry to store and recreate the optical fields of an object has been used to visualize the amplitudes of displacement of various vibrational modes of a graphite/epoxy plate. Indications of anomalous displacements have enabled the detection of barely visible impact damage in the graphite/epoxy plate. The theoretical background to the formation of the fringe-contoured images of the vibrating specimen has been presented.

REFERENCES

1. Heller, M. and Rumble, S.J. Dynamic response of a graphite/epoxy composite plate. Aero. Res. Labs. Structures Tech. Memo. No. 438, May 1986.

2. Rumble, S.J. Introduction to holographic interferometry applied to strain determination. Aero. Res. Labs Structures Tech. Memo. No. 443, June 1986.

3. Hariharan, P. Optical Holography. Principles, techniques and applications. First edition. Melbourne: Cambridge University Press, 1984.

4. Vest C.M. Holographic Interferometry. First edition. Brisbane: John Wiley and Sons, 1979.

5. Erf, R.K. Holographic non-destructive testing. London: Academic Press, 1974.

6. Neumann, D.B., Jacobson, C.F. and Brown, G.M. Holographic techniques for determining the phase of vibrating objects. Applied Optics 9(6) June 1970, pp 1357-1362.

7. Levitt, J.A. and Stetson, K.A. Mechanical vibrations: mapping their phase with hologram interferometry. Applied Optics 15(1) Jan. 1976, pp 195-199.

8. Hariharan, P. and Oreb, B.F. Stroboscopic holographic interferometry: application of digital techniques. Optics Commun. 59(2) Aug. 1986, pp 83-86.

APPENDIX I – Brief theory of time-averaged holographic interferometry

Consider an object illuminated with monochromatic, coherent light. The resultant electric field E at any given point will be varying sinusoidally at a single frequency and with constant amplitude and phase. It can also be correlated with other points in the optical field. This variation can be expressed as follows:

$$E(x,y,z) = E_o(x,y,z)\cos(2\pi\upsilon t - \phi(x,y,z)). \tag{A.1}$$

The single frequency nature of the light enables a complex amplitude notation to be used for the electric field. This has the form

$$E(x,y,z,t) = |E(x,y,z)| \exp\{-i\phi(x,y,z)\}. \tag{A.2}$$

This notation will be used in the following discussion.

Consider an object illuminated with monochromatic, coherent light and which is vibrating in a mode with angular frequency ω. Let the complex amplitude due to the scattered light from a general point Q(l,m) on the vibrating object and at time t be as follows:

$$\begin{aligned} O(l,m,t) &= |O(l,m)| \exp\{-i[\Phi(l,m) + \Theta(l,m,t)]\}, \\ &= O(l,m)\exp\{\Theta(l,m,t)\} \end{aligned} \tag{A.3}$$

where $O(l,m) = |O(l,m)| \exp\{-i\Phi(l,m)\}$ would be the complex amplitude of the stationary object, and $\Theta(l,m,t)$ contains the time dependence of the complex amplitude phase which arises due to the vibration of the object. The Θ term can be defined as follows:

$$\Theta(l,m,t) = -\underset{\sim}{k}_1 \cdot \underset{\sim}{d}(l,m,t), \tag{A.4}$$

where $\underset{\sim}{k}_1$ is the propagation vector of the incident light and $\underset{\sim}{d} = \underset{\sim}{d}_o(l,m)\sin(\omega t + \phi_o)$ is the displacement of a general point Q(l,m) on the object vibrating with angular frequency ω, phase ϕ_o and amplitude $\underset{\sim}{d}_o$.

Let the complex amplitude at a photographic plate (in the x,y plane), due to the scattered light from a general point Q(l, m) be given by

$$o(x,y,l,m,t) = \mid o(x,y,l,m) \mid \exp\{-i[\phi(x.t,l,m) + \Theta(x,y,l,m,t)]\}, \quad (A.5)$$

where $\mid o(x,y,l,m) \mid \exp\{-i\phi(x,y,l,m)\}$ would be the complex amplitude due to the stationary object, and $\Theta(x,y,l,m,t)$ contains the time dependence of the complex amplitude phase. The Θ term can be defined as follows:

$$\Theta(x,y,l,m,t) = \underset{\sim}{K}\,(\underset{\sim}{k}_1,\underset{\sim}{k}_2).\underset{\sim}{d}\,(l,m,t), \quad (A.6)$$

where $\underset{\sim}{K} = \underset{\sim}{k}_2 - \underset{\sim}{k}_1$ is the sensitivity vector, $\underset{\sim}{k}_2$ and $\underset{\sim}{k}_1$ are respectively the propagation vectors of the incident and scattered light, and $\underset{\sim}{d}$ has been defined above.

If in addition to the object field, a plane wave is allowed to fall at an angle γ to the photographic plate, then the variation of the complex amplitude due to this beam is

$$r(x,y) = r \exp\{i2\pi\zeta x\}, \quad (A.7)$$

where $\zeta = \sin(\gamma)/\lambda$, and λ is the wavelength of the monochromatic illumination. This beam is called the reference beam.

The photographic plate responds to the intensity of the superposition of these two fields. The resultant intensity at the plate due to point Q(l,m) and at time t is

$$\begin{aligned} I(x,y,t) &= \mid o(x,y,t) + r(x) \mid^2, \\ &= \mid o \mid^2 + \mid r \mid^2 + or^* + ro^*, \end{aligned} \quad (A.8)$$

(r^* and o^* are the complex conjugates of r and o respectively).

Consider initially that the photographic plate is exposed to this intensity distribution at a fixed time. If the photographic plate is processed so that its amplitude transmittance t(x,y) is linearly related to intensity then it can be shown (see for example reference 3) that it is the or* term in the above expression that is responsible for the reconstruction of the original object field at the plate. The reconstruction occurs when the developed photographic plate or hologram is illuminated with the same reference beam that was used to expose it. The complex amplitude of the transmitted or reconstructed wave u(x,y) is then given by

$$\begin{aligned} u(x,y) &= t(x,y)r(x,y), \\ &= \alpha_1 o(x,y)r^*(x,y)r(x,y), \\ &= \alpha_1 o(x,y)r^2, \\ &= \alpha_2 o(x,y), \end{aligned} \tag{A.9}$$

where α_1 and α_2 are constants. Equation A.9 shows that the reconstructed wave u(x,y) at the photographic plate is proportional to the object wave o(x,y) that was present during the exposure. Thus an optical imaging system will form the same image when viewing the original wave o(x,y) or the reconstructed wave u(x,y).

The discussion in the above paragraph concerns the case at a fixed time. In the case of a vibrating object, the intensity distribution at the photographic plate will be varying with time due to the phase variations of the object field. However, the electric field of the object beam will vary much more rapidly than the phase variation due to the vibration of the object. The resultant intensity distribution on the photographic plate can thus be considered to be the sum of many intensity distributions, each recorded at slightly different object positions. Therefore the reconstructed wave will enable the formation of an image that will be the time average of many images reconstructed by holograms each recorded at slightly different object positions. Thus, if a hologram that has been recorded as the object is vibrating, is viewed by an optical system, then the image formed will correspond to an object with the scattered amplitudes equivalent to the time-average of the scattered amplitudes of the vibrating object. The effective scattering amplitude O (l,m) from the vibrating object will have the following form

$$O(l,m) = \frac{1}{T} \int_0^T | O(l,m) | \exp\{-i[\phi(l,m) + \theta(l,m,\underset{\sim}{K},t)]\}dt, \tag{A.10}$$

where

$$\theta\ (l,m,\underset{\sim}{K},t) = \underset{\sim}{K}\ (\underset{\sim}{k}_1,\underset{\sim}{k}_2).\underset{\sim}{d}\ (l,m,t), \tag{A.11}$$

and T is the exposure time. Thus

$$\begin{aligned} O\ (l,m) &= |\ O(l,m)\ |\ \exp\{-i\Phi(l,m)\}\ \frac{1}{T}\ \int_o^T\ \exp\{-i\underset{\sim}{K}.\underset{\sim}{d}\ \}dt, \\ &= O(l,m)M_T(\underset{\sim}{K}\ .\underset{\sim}{d}\ ), \end{aligned} \tag{A.12}$$

where M_T is known as the characteristic function. This equation indicates that the equivalent object to the image formed in a time-averaged hologram is a function of the viewing direction due to the dependence of the characteristic function on the sensitivity vector $\underset{\sim}{K}$. If the exposure time is long compared to the period of vibration ($T >> 2\pi/\omega$) then the characteristic function M_T can be expressed as follows

$$\begin{aligned} M_T(\underset{\sim}{K}\ .\underset{\sim}{d}) &= \lim_{T\to\infty}\ \frac{1}{T}\ \int_o^T\ \exp[-i\underset{\sim}{K}\ .\underset{\sim}{d}_o(l,m)\sin(\omega t + \phi_o)]dt, \\ &= J_o[\underset{\sim}{K}\ .\underset{\sim}{d}_o(l,m)], \end{aligned} \tag{A.13}$$

where J_o is the zero-order Bessel function of the first kind. The intensity in the reconstructed image is then

$$\begin{aligned} I(l,m) &\approx |\ O\ (l,m)M_T(l,m)\ |^2, \\ &\approx I_o(x,y)J_o^2[\underset{\sim}{K}\ .\underset{\sim}{d}_o(l,m)], \end{aligned} \tag{A.14}$$

where I_o is the intensity of the stationary object.

PHASE MODULATION OF THE REFERENCE BEAM

Consider a case where the phase of the reference beam used to record the hologram is modulated at the frequency of vibration. This modulation can be simply accomplished by incorporating in the reference beam path a reflection from a mirror mounted on a piezoelectric translator.

In this situation equation A.7 becomes

$$\begin{aligned} r(x,y,t) &= r\exp\{i[2\pi\zeta x + \phi_r(t)]\} \\ &= r(x,y)\exp\{i\phi_r(t)\}, \end{aligned} \tag{A.15}$$

where $\phi_r(t) = \phi_{ro}\sin(\omega t + \delta)$ and ϕ_{ro} is the amplitude of the phase modulation and δ is the phase of the modulation relative to some point on the vibrating object. The resultant intensity at the photographic plate due to the general point Q(l,m) and at time t is

$$\begin{aligned} I(x,y,t) &= |\, o(x,y,t) + r(x,y,t)\,|^2, \\ &= |\, o\,|^2 + |\, r\,|^2 + or^* + ro^*, \end{aligned} \tag{A.16}$$

As stated previously the or* term is responsible for the reconstruction of the original object field at the plate. This term is given by

$$\begin{aligned} or^* &= o(x,y,t)r^*(x,y,t), \\ &= |\, o(x,y)\,|\exp\{-i[\phi(x,y) + \theta(x,y,t)]\}r\exp\{i[2\pi\zeta x + \phi_r(t)]\} \\ &= |\, o(x,y)\,|\exp\{-i[\phi(x,y) + \theta(x,y,t) + \phi_r(t)]\}r\exp\{i2\pi\zeta x\}. \end{aligned} \tag{A.17}$$

This shows that the effect of the modulated reference beam can be considered to be an additional phase variation of the scattered light from the object.

On reconstruction, an unmodulated reference beam is used. Thus, following the previous arguments which lead to equation A.10, the equivalent object will now be given by

$$O(l,m) = \frac{I}{T} \int_0^T |O(l,m)| \exp\{-i[\Phi(l,m) + \theta(l,m,\underset{\sim}{K},t) + \phi_r(t)]\}dt,$$

$$= O(l,m) \frac{I}{T} \int_0^T \exp\{-i[\theta(l,m,\underset{\sim}{K},t) + \phi_r(t)]\}dt, \tag{A.18}$$

Now as

$$\theta(l,m,\underset{\sim}{K},t) + \phi_r(t) = \underset{\sim}{K} \cdot \underset{\sim}{d}_o \sin(\omega t + \phi_o) + \phi_{ro} \sin(\omega t + \delta), \tag{A.19}$$

$$= [(\underset{\sim}{K} \cdot \underset{\sim}{d}_o)^2 + \phi_{ro}^2 + 2\underset{\sim}{K} \cdot \underset{\sim}{d}_o \phi_{ro} \cos(\phi_o - \delta)]^{1/2} \sin(\omega t + \beta),$$

then O (l,m) can be written as *follows*

$$O(l,m) = O(l,m) M_T \tag{A.20}$$

where

$$M_T = J_o\{[(\underset{\sim}{K} \cdot \underset{\sim}{d}_o)^2 + \phi_{ro}^2 + 2\underset{\sim}{K} \cdot d_o \phi_{ro} \cos(\phi_o - \delta)]^{1/2}\}. \tag{A.21}$$

The intensity in the reconstructed image is then

$$I(l,m) = I_o(l,m) J_o^2\{[(\underset{\sim}{K} \cdot \underset{\sim}{d}_o)^2 + \phi_{ro}^2 + 2\underset{\sim}{K} \cdot \underset{\sim}{d}_o \phi_{ro} \cos(\phi_o - \delta)]^{1/2}\}. \tag{A.22}$$

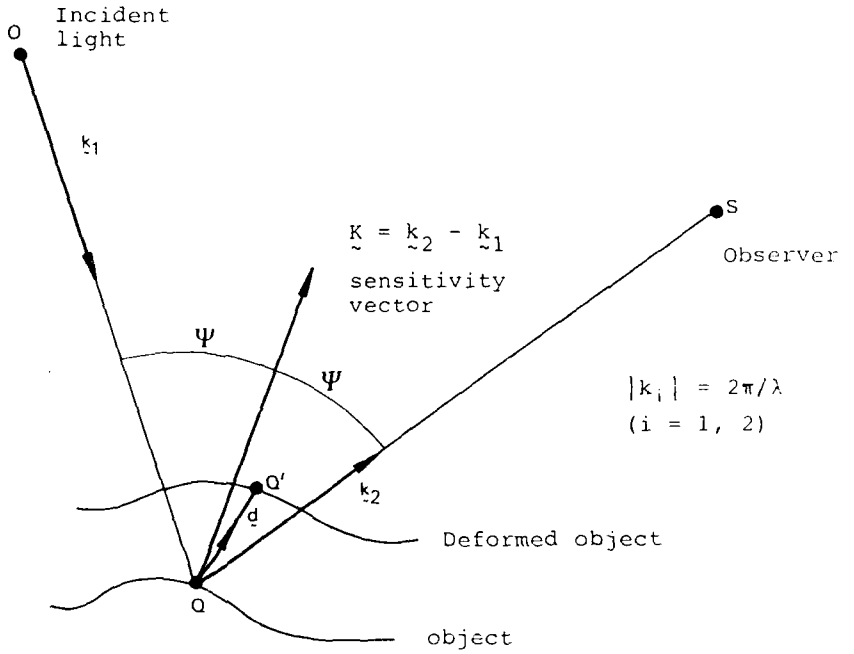

FIG. 1 OPTICAL ARRANGEMENT DEFINING SENSITIVITY VECTOR

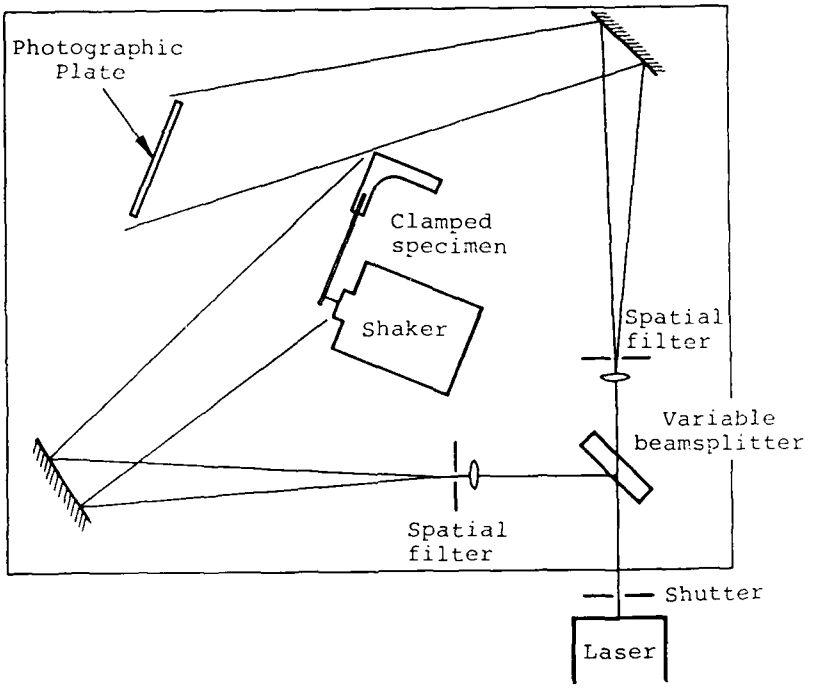

FIG. 2. SCHEMATIC DIAGRAM OF OPTICAL ARRANGEMENT

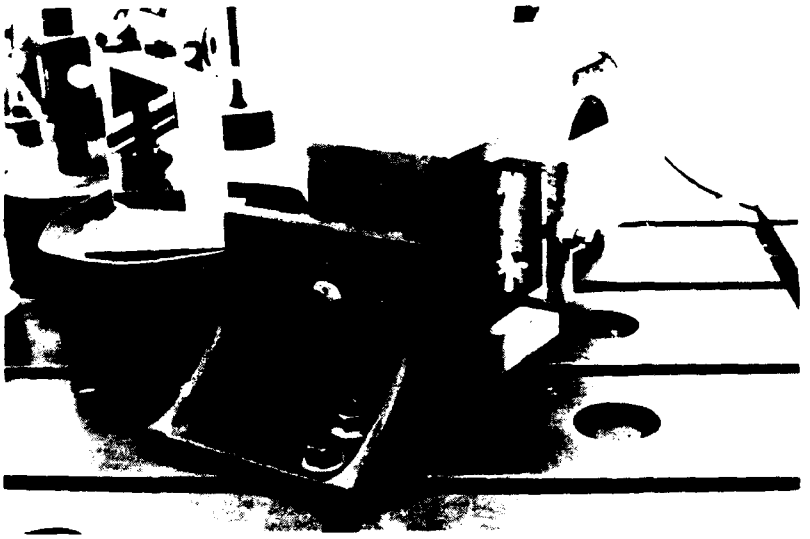

FIG. 3. SPECIMEN CLAMPING ARRANGEMENT

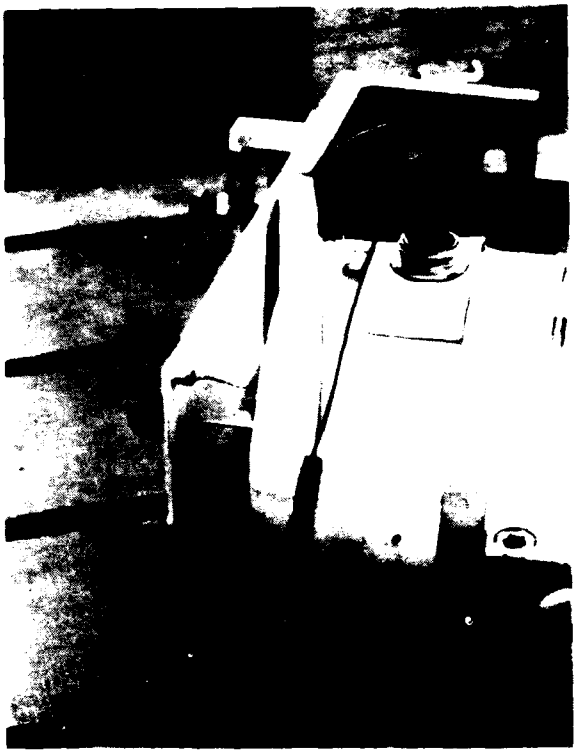

FIG. 4. SPECIMEN EXCITATION ARRANGEMENT

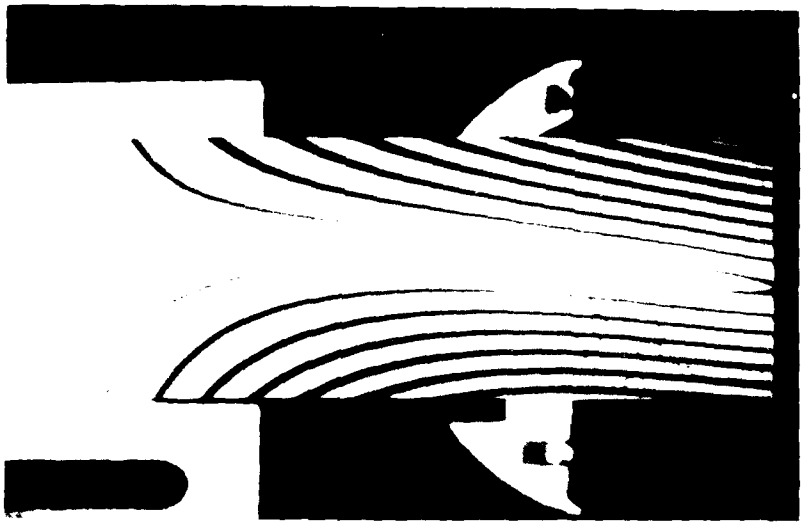

FIG. 5. HOLOGRAM AT 434 Hz FOR UNDAMAGED SPECIMEN

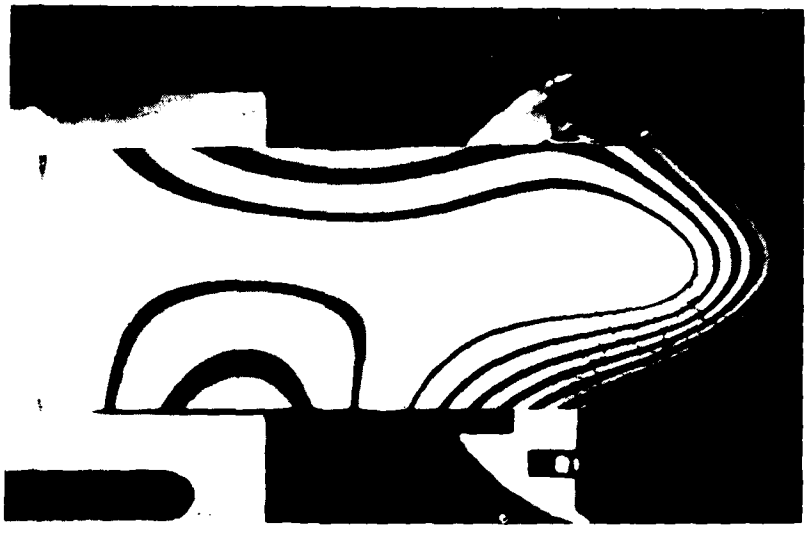

FIG. 6. HOLOGRAM AT 1125 Hz FOR UNDAMAGED SPECIMEN

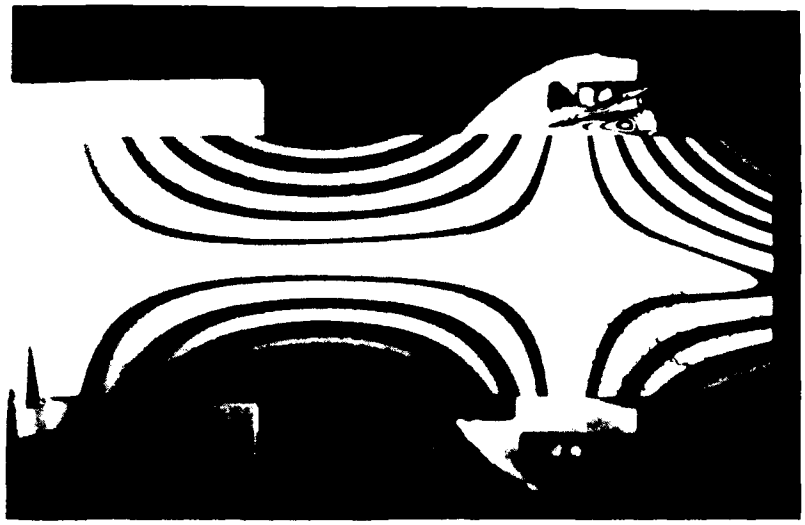

FIG. 7. HOLOGRAM AT 1530 Hz FOR UNDAMAGED SPECIMEN

FIG. 8. HOLOGRAM AT 2100 Hz FOR UNDAMAGED SPECIMEN

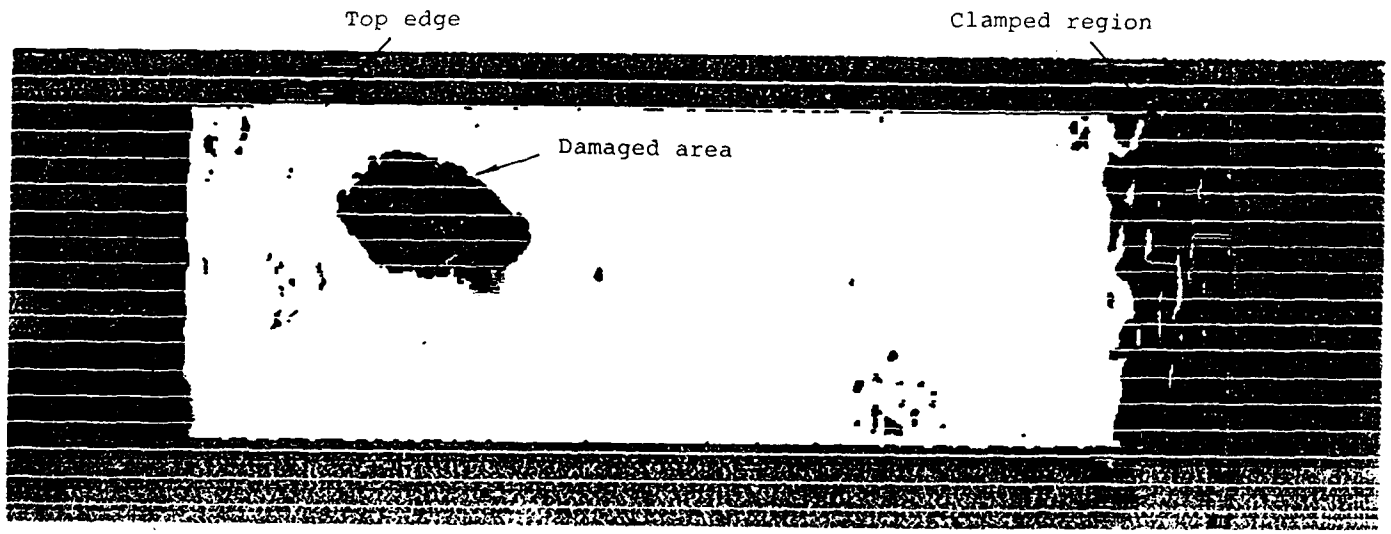

FIG. 9. C-SCAN OF SPECIMEN AFTER IMPACT DAMAGE AT 0.9 OF SAMPLE THICKNESS

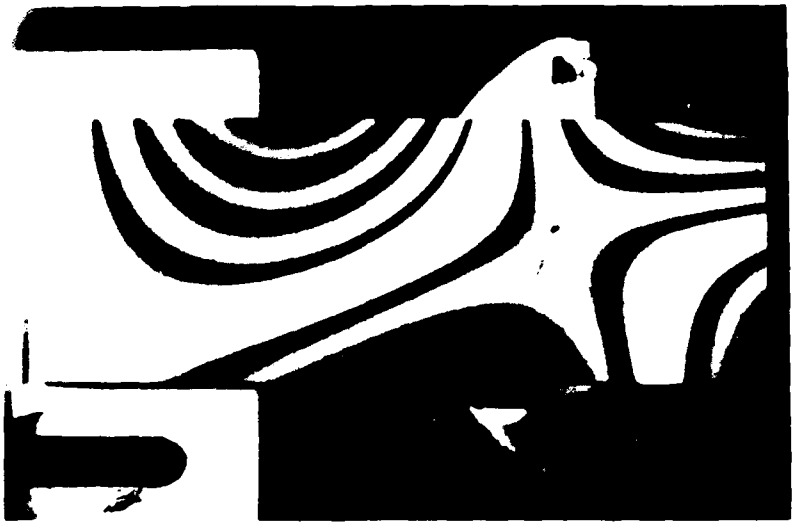

FIG. 10. HOLOGRAM AT 1157 Hz FOR DAMAGED SPECIMEN

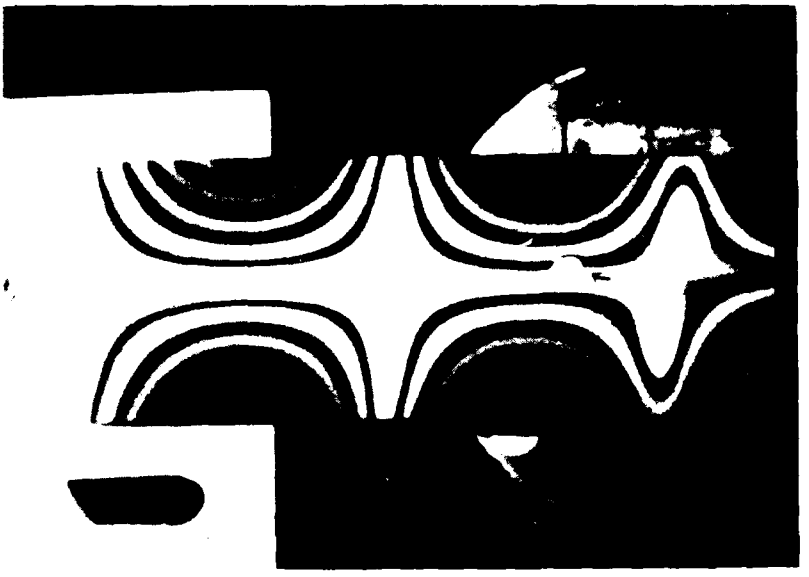

FIG. 11. HOLOGRAM AT 2160 Hz FOR DAMAGED SPECIMEN

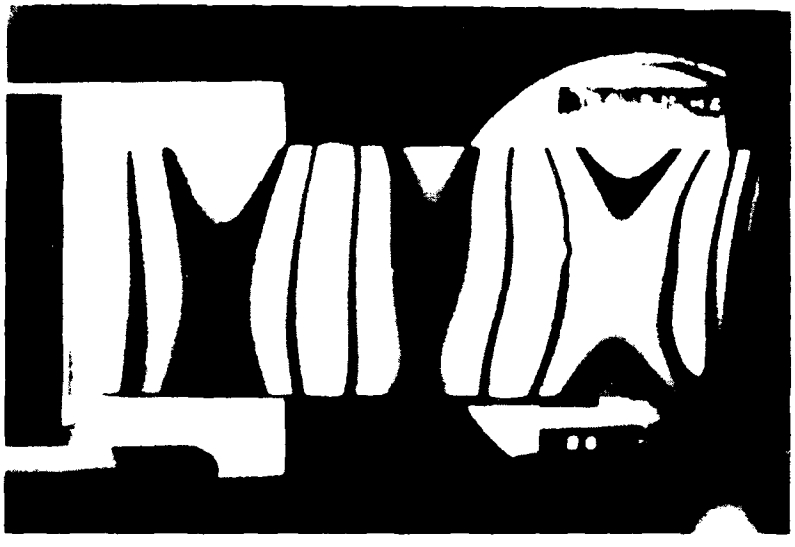

FIG. 12. HOLOGRAM AT 2340 Hz FOR DAMAGED SPECIMEN

FIG. 13. ARRANGEMENT OF OPTICAL COMPONENTS

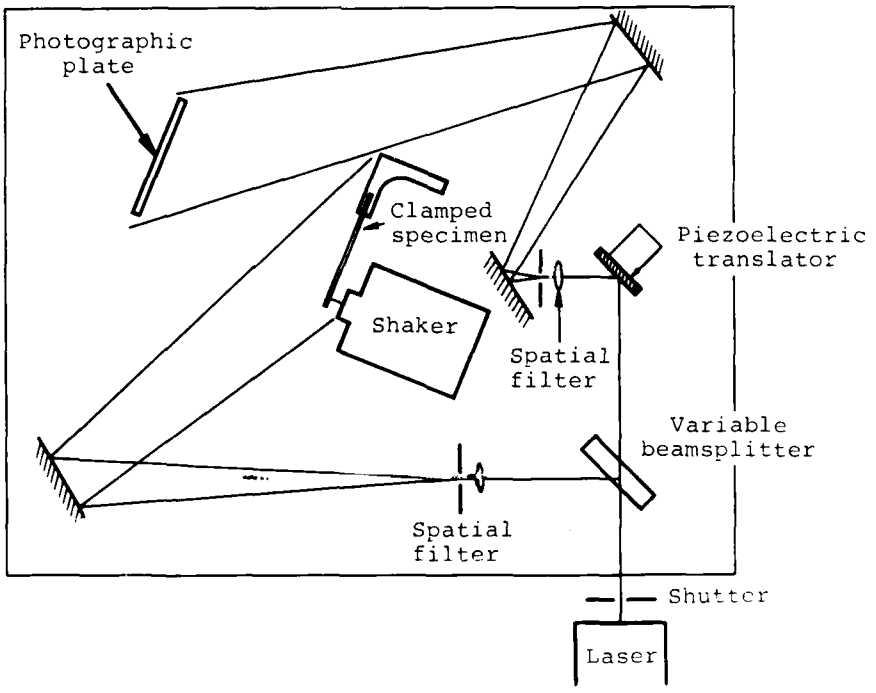

FIG. 14. SCHEMATIC DIAGRAM OF OPTICAL ARRANGEMENT

FIG. 15. HOLOGRAM AT 1157 Hz FOR DAMAGED SPECIMEN AND WITH TEMPORAL MODULATION OF REFERENCE BEAM. ZERO PHASE DIFFERENCE BETWEEN PIEZOELECTRIC TRANSLATOR AND ACCELEROMETER

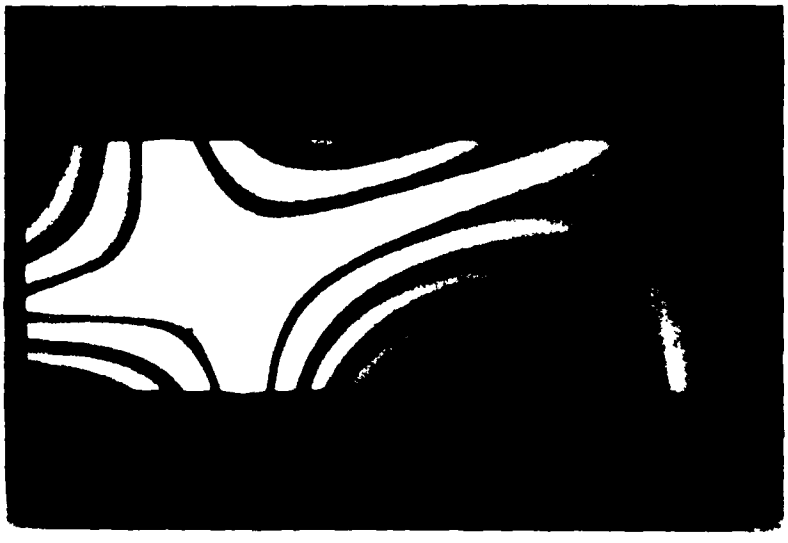

FIG. 16. HOLOGRAM AT 1157 Hz FOR DAMAGED SPECIMEN AND WITH TEMPORAL MODULATION OF REFERENCE BEAM. 180° PHASE DIFFERENCE BETWEEN PIEZOELECTRIC TRANSLATOR AND ACCELEROMETER

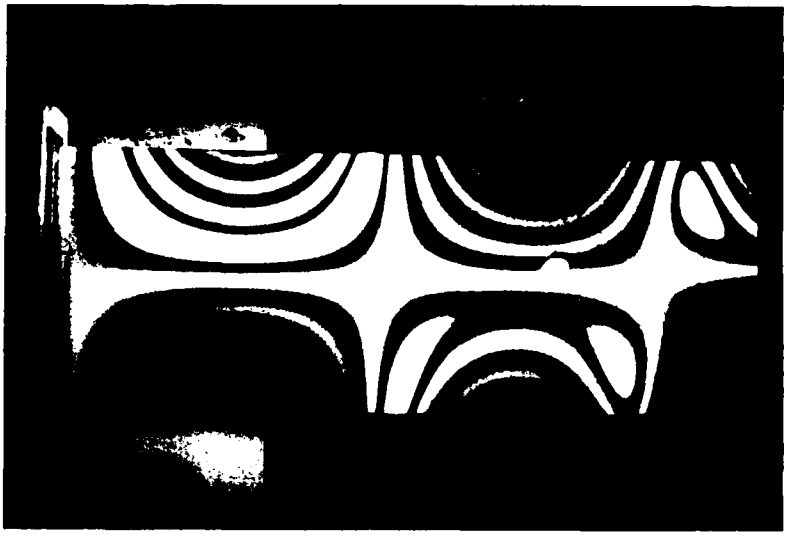

FIG. 17. HOLOGRAM AT 2160 Hz FOR DAMAGED SPECIMEN AND WITH TEMPORAL MODULATION OF REFERENCE BEAM. ZERO PHASE DIFFERENCE BETWEEN PIEZOELECTRIC TRANSLATOR AND ACCELEROMETER

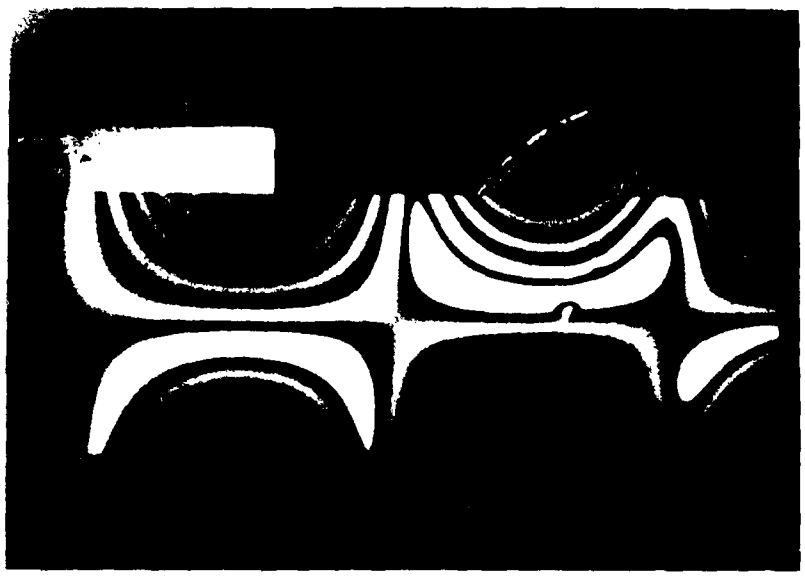

FIG. 18. HOLOGRAM AT 2160 Hz FOR DAMAGED SPECIMEN AND WITH TEMPORAL MODULATION OF REFERENCE BEAM. 180° PHASE DIFFERENCE BETWEEN PIEZOELECTRIC TRANSLATOR AND ACCELEROMETER

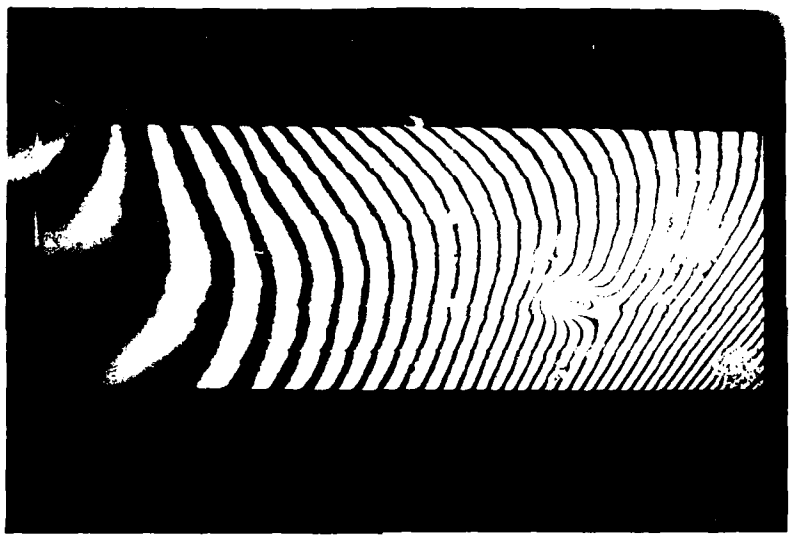

FIG. 19. DOUBLE EXPOSURE HOLOGRAM OF THE BACK FACE OF THE DAMAGED SPECIMEN, USING THERMAL STRESSING

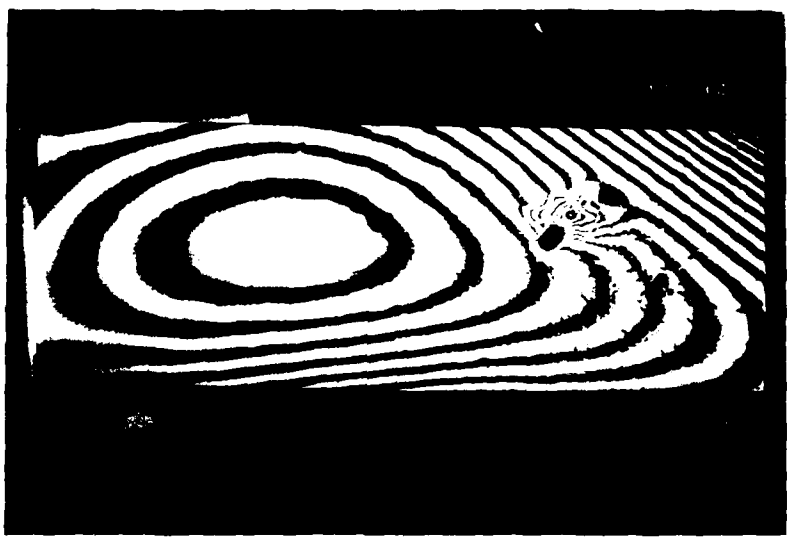

FIG. 20. DOUBLE EXPOSURE HOLOGRAM OF THE FRONT FACE OF THE DAMAGED SPECIMEN, USING THERMAL STRESSING

DISTRIBUTION

AUSTRALIA

Department of Defence

Defence Central
- Chief Defence Scientist
- Assist Chief Defence Scientist, Operations (Shared Copy)
- Assist Chief Defence Scientist, Policy (Shared Copy)
- Director, Departmental Publications
- Counsellor, Defence Science, London (Doc Data sheet only)
- Counsellor, Defence Science, Washington (Doc Data sheet only)
- SA to the Thailand Military R and D Centre (Doc Data sheet only)
- SA to the DRC (Kuala Lumpur) (Doc Data sheet only)
- OIC TRS, Defence Central Library
- Document Exchange Centre, DISB (18 copies)
- Joint Intelligence Organisation
- Librarian H Block, Victoria Barracks, Melbourne
- Director General - Army Development (NSO) (4 copies)
- Defence Industry and Materiel Policy, FAS

Aeronautical Research Laboratories
- Director
- Library
- Divisional File - Structures
- Author: S.J. Rumble
- J. Sparrow
- B. Lawrie
- J. Gordon
- M. Heller

Materials Research Laboratories
- Director/Library

Defence Science & Technology Organisation - Salisbury
- Library

WSRL
- Maritime Systems Division (Sydney)

Navy Office
- Navy Scientific Adviser (3 copies Doc Data sheet)

Army Office
- Scientific Adviser - Army (Doc Data sheet only)
- Engineering Development Establishment, Library

Air Force Office
- Air Force Scientific Adviser (Doc Data sheet only)

Department of Transport & Communication
- Library

SPARES (10 copies)
TOTAL (50 copies)

AL 149
REVISED APRIL 87

DEPARTMENT OF DEFENCE

DOCUMENT CONTROL DATA

PAGE CLASSIFICATION
UNCLASSIFIED

PRIVACY MARKING
–

1a. AR NUMBER	1b. ESTABLISHMENT NUMBER	2. DOCUMENT DATE	3. TASK NUMBER
AR-004-549	ARL-STRUC-TM-467	25 AUGUST 1987	DST 83/005

4. TITLE
EXPERIMENTAL ASPECTS OF USING TIME-AVERAGED HOLOGRAPHIC INTERFEROMETRY TO DETECT BARELY VISIBLE IMPACT DAMAGE IN A GRAPHITE/EPOXY COMPOSITE PLATE

5. SECURITY CLASSIFICATION
(PLACE APPROPRIATE CLASSIFICATION IN BOX (S) IE. SECRET (S), CONFIDENTIAL (C), RESTRICTED (R), UNCLASSIFIED (U).)

DOCUMENT	TITLE	ABSTRACT
U	U	U

6. No. PAGES
32

7. No. REFS.
8

8. AUTHOR(S)
S.J. RUMBLE

9. DOWNGRADING/DELIMITING INSTRUCTIONS
NOT APPLICABLE

10. CORPORATE AUTHOR AND ADDRESS

AERONAUTICAL RESEARCH LABORATORIES
P.O. BOX 4331, MELBOURNE VIC. 3001

11. OFFICE/POSITION RESPONSIBLE FOR
SPONSOR –
SECURITY –
DOWNGRADING –
APPROVAL –

12. SECONDARY DISTRIBUTION (OF THIS DOCUMENT)
Approved for public release

OVERSEAS ENQUIRIES OUTSIDE STATED LIMITATIONS SHOULD BE REFERRED THROUGH ASDIS, DEFENCE INFORMATION SERVICES BRANCH, DEPARTMENT OF DEFENCE, CAMPBELL PARK, CANBERRA, ACT 2601

13a. THIS DOCUMENT MAY BE ANNOUNCED IN CATALOGUES AND AWARENESS SERVICES AVAILABLE TO.....
No limitations

13b. CITATION FOR OTHER PURPOSES (IE. CASUAL ANNOUNCEMENT) MAY BE [X] **UNRESTRICTED OR** [ ] **AS FOR 13a.**

14. DESCRIPTORS
Holographic interferometry
Graphite-epoxy laminates
Impact damage
Nondestructive testing

15. DRDA SUBJECT CATEGORIES
0071F
0094J

16. ABSTRACT

Time-averaged holographic interferometry has been used to detect barely visible impact damage in a graphite/epoxy plate. Details are given of both the experimental and theoretical aspects of time-averaged holographic interferometry, including temporal modulation of the laser light. Double exposure holographic interferometry has also been used to detect barely visible impact damage.

PAGE CLASSIFICATION
UNCLASSIFIED
PRIVACY MARKING

THIS PAGE IS TO BE USED TO RECORD INFORMATION WHICH IS REQUIRED BY THE ESTABLISHMENT FOR ITS OWN USE BUT WHICH WILL NOT BE ADDED TO THE DISTIS DATA UNLESS SPECIFICALLY REQUESTED.

16. ABSTRACT (CONT.)

17. IMPRINT

AERONAUTICAL RESEARCH LABORATORIES, MELBOURNE

18. DOCUMENT SERIES AND NUMBER	19. COST CODE	20. TYPE OF REPORT AND PERIOD COVERED
STRUCTURES TECHNICAL MEMORANDUM 467	27 1055	

21. COMPUTER PROGRAMS USED

22. ESTABLISHMENT FILE REF. (S)

23. ADDITIONAL INFORMATION (AS REQUIRED)

END

DATE
FILMED

8 88